The Nernst-Ettingshausen, Seebeck and Hall Effects in $(Sb_{1-X}Bi_X)_2Te_3$ Single Crystals

[1] M. K. Zhitinskaya, [1]S. A. Nemov, [1]Yu.G.Ispolov, [2]T. E. Svechnikova
State Politechnical University, St-Petersburg ,
Politechnicheskaya, 29, St.Petersburg, 195251, Russia
2. Baikov Institute of Metallurgy and Materials Sciences, Moscow
[1]nym@online.ru

Abstract

We report the results on measurement of the temperature dependences of transport coefficients: Nernst-Ettingshausen (Q_{123}), Hall (R_{123}, R_{321}), Seebeck (S_{11}) and electroconductivity (σ_{11}) in single crystals of solid solutions $(Sb_{1-X}Bi_X)_2Te_3$. All measurements were made on high-quality Czochralski-grown single crystals in temperature interval 77 – 400 K. It was shown that the main features of the experiment data can be explained within two-band model. The estimates of the band-gap width ε_g and the energy gap $\Delta\varepsilon_v$ between the main and additional valence-band extrema for Sb_2Te_3: $\varepsilon_g \approx 0.3$ eV, $\Delta\varepsilon_v \approx 0.1$eV and for $Sb_{1.5}Bi_{0.5}Te_3$ $\varepsilon_g \approx 0.12$ eV, $\Delta\varepsilon_v \approx 0.02$ eV) were made.

Introduction

Sb_2Te_3 and solid solutions $Sb_{1.5}Bi_{0.5}Te_3$ are part of crystals family $(Sb_{1-X}Bi_X)_2Te_3$. and they are employed as a high-efficiency room-temperature thermoelectric materials. This accounts for its application potential and the intense interest expressed in it by researches. However, despite the wealth of literature data available, the character of its band structure and hole mechanism of scattering remain a subject of debate.

The family of crystals $(Sb_{1-X}Bi_X)_2Te_3$ are narrow-band-gap semiconductos. They belong to the class of layered compounds and are characterized by the presence of a large number of intrinsic acceptor-type defects; this factorcomplicates the study of the Sb_2Te_3 and solid solutions $Sb_{1.5}Bi_{0.5}Te_3$. In this work, the scope of the transport phenomena studied is broadened. We studied the Nernst-Ettingshausen effect (TNEE) together with the Seebeck and Hall effects and their temperature and concentration dependences.

Samples

The composition of the samples is described by the chemical formula $(Sb_{1-x}Bi_x)_2Te_{3-y}Se_y$, where $x = 0$ and 0.25; $y = 0$; 0.09 and 0.012 (x = 0.01 corresponds to $6*10^{19}cm^{-3}$).

- All crystals were grown by Czochralski technique with replenishment of the melt from a liquid phase.
- The homogeneity and perfection of crystals was verified by scaned electron microscope
- The homogeneity of impurity distribution along the samples was estimated by measuring of Seebeck coefficient with the aid of a thermoprobe at 300 K.

Experiment

On each sample, the following independent transport components were measured: the Seebeck coefficients S_{11} and S_{33}, the Hall coefficients R_{123} and R_{321}, the Nernst-Ettingshausen constant Q_{123}, and electrical conductivity σ11. In this notation the number 3 indicates the trigonal axis of a crystal. The subscripts of the coefficients represent the following, in the order they appeared: the first is used for the direction of the measured electric field, the second for the direction of the electric current or the temperature gradient, and the third for the magnetic field direction. The Hall and TNEE were studied using techniques that permitted one to reduce to a minimum the effect of their parasitic nonisothermal components, which may make up a noticeable fraction of the measured effect in thermoelectric materials.

The measurements were carried out mainly in the temperature range 77 - 420 K. The carrier density was derived from the larger component of the Hall tensor R_{321} at 77 K using the expression $n, p = [q\, R_{321}(77\text{ K})]^{-1}$.

The Nernst-Ettingshausen Effect. Theory.

The complex studying of the Nernst-Ettingshausen effect (TNEE) together with the Seebeck and Hall effects and their temperature and concentration dependences we used to find (determine) the parameters of energy spectrum: hole density-of-states effective mass m_d, electron scattering parameter r, fundamental energy gap ε_g or energy gap among two additional zone $\Delta\varepsilon$. A computer simulation of the Hall and Seebeck coefficients were carried out in the context of the two-band zone.

The density-of-states effective mass

A calculation of the density-of-states effective mass of hole m_d for strongly degenerate statistic was carried out using the expression:

$$m_d / m_e = \frac{e}{k_0} \cdot \frac{\left(3\pi^2 n\right)^{\frac{2}{3}}}{k_0 T} \cdot \left(\frac{\hbar}{\pi}\right)^2 \left(S_{11} - \frac{Q_{123}}{R_{123}\sigma_{11}}\right) \quad (1)$$

where k_0 -Bolzman's constant, e - charge of electron.

Mehanism of scattering.

The estimation of the electron scattering parameter from the set of kinetic coefficients: Q_{123}, S_{11}, R_{123} σ_{11} is given by the expression: $\frac{Q_{123}}{S_{11} * R_{123} * \sigma_{11}} = \frac{r - 0.5}{r + 1}$, where r – electron scattering parameter in an expression $\tau = \tau_0 * \varepsilon^{r-1/2}$.

Energy gap ε_g

At high temperatures (for Sb_2Te_3 T > 500 K and for $Sb_{1.5}Bi_{0.5}Te_3$ T.>300 ÷ 400 K), the contribution from the minority carriers to the transport phenomena becomes noticeable and grows rapidly with temperature. In the simplest case of a valence band consisting of only one subband, the

Q_{123} coefficient in the region of mixed electron-hole conduction has the form

$$Q = \sigma_p / \sigma Q_p + \sigma_n / \sigma Q_n + Q_{np}, \quad (2)$$

where Q_p, Q_n, Q_{np} and σ are described

$$eQ_n / k_0 = R_{123}\sigma_{11}(r - 1/2), \quad (3)$$

$$\sigma = \sigma_n + \sigma_p \quad (4)$$

$$Q_{np} = \frac{\sigma_n \sigma_p}{\sigma^2}(S_p - S_n)(u_n + u_p), \quad (5)$$

u_p and u_n are the corresponding Hall mobilities of the holes and electrons. At the beginning of mixed conductivity, where the concentration of the minority carriers (electrons in this case) is still low, i.e., for $\sigma_n \ll \sigma_p$ Eq.(5) assumes the form

$$eQ_{np} / k_0 \approx \sigma_n / \sigma(S_p - S_n)(u_p + u_n) \approx n \approx \exp(-\varepsilon_g / k_0 T) \quad (6)$$

(ε_g is the band-gap width). The mixed term Q_{np} is always positive and proportional to the electron contributionto the conductivity, which, in turn, is proportional to the electron concentration *n*. As a result, the measured negative coefficient Q, according to Eqs.(3)-(7),passes through a minimum and thereafter starts to decrease rapidly in absolute value and tends to sign reversal.

Energy gap among two additional zone Δε.

The Nernst-Ettingshausen effect can be used for determination of the energy gap among two additional band. In the temperature range where the carriers of the additional band just begin to contribute and the ratio of the hole concentration in the second band p_2 to the total hole concentration $p_0 = p_1 + p_2$ is $\nu = p_2 / p_0 \ll 1$. In this case,Eq.6 is

$$eQ_{123}^{(1,2)} / k_0 \approx [S_{11}^{(1)} - S_{11}^{(2)}][A_c^{(1)} u_a^{(1)} + A_c^{(2)} u_{a\ n}^{(2)}] t_a^{(1)} t_a^{(2)} \approx p_2 / p_0 \approx \exp(-\Delta\varepsilon_v / k_0 T), \quad (7)$$

where $\Delta\varepsilon_v$ is the energy gap between the valence bands, $t_a^{(1)}$ and $t_a^{(2)}$ are expressed with formula:

$$t_a^{(1)} = \sigma_a^{(1)}[\sigma_a^{[1]} + \sigma_a^{[2]}]$$
$$t_a^{(2)} = \sigma_a^{(2)}[\sigma_a^{[1]} + \sigma_a^{[2]}] \quad (8)$$

Results and discussion

Our results on the anisotropy and temperature dependences of the Hall and Seebeck coefficients and the electrical conductivity agree well with the literature data. So main attention is focused, in this paper, on the transport coefficients that are less covered in the literature, namely, the Nernst-Ettingshausen effect and anisotropy in the Seebeck coefficient.

All the Sb_2Te_3 and $Sb_{1.5}Bi_{0.5}Te_3$ samples studied exhibited the following characteristic features in the temperature dependences:

(i) A negative sign of the Nernst-Ettingshausen coefficient Q_{123} throughout the temperature range covered (Fig.1).

(ii) The Seebeck coefficient is isotropic (whitin the experimental accuracy) in the low-temperature region (near100 K) and reveals, for T > 140 , an anisotropy ΔS = $S_{33} - S_{11}$, which grows with temperature.

(iii) The Hall tensor components R_{123} and R_{321} for Sb_2Te_3 crystals grow with temperature at different rates; this is accompanied by a decrease in the Hall coefficient anisotropy and a crossing of its components near 300 K (Fig.2)

Sb_2Te_3

The experimental results of the transverse Nernst-Ettingshausen tensor components and of the Seebeck coefficients of Sb_2Te_3 crystals are presented on the Fig.1,2.

The experimental results were used for estimation of the parameters of valence band of the Sb_2Te_3. The particularities of the temperature dependences of kinetic coefficients: the increase and crossing of the components R_{ijk}, negative magnitude Q and its increasing with rising temperature, anisotropy of S_{ii} are observed in the interval 200 < T < 500 K. For explanation of these dependences we used the two subband model. The estimation of the energy gap between these bands gived the value $\Delta\varepsilon_v \approx 0,1eV$.

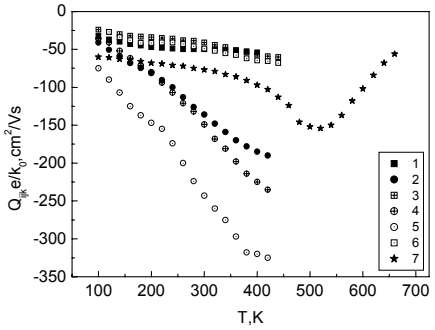

Fig.1. Temperature dependences Q_{ijk} for monocrystalls of Sb_2Te_3

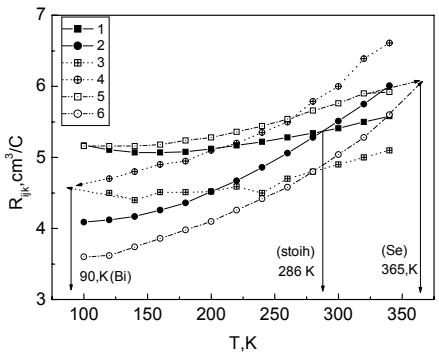

Fig. 2. Temperature dependences R_{ijk} for monocrystalls of Sb_2Te_3

And we have to assume that the carriers of the second subband have effective mass much more smaller than effective mass of the first subband and the mobility of 2-subband holes is larger of 1-subband holes.

An analysis of the experimental data for Sb_2Te_3, obtained at the onset of the intrinsic conductivity yielded an estimate of the thermal energy gap between the valence and conduction bands extrapolated to zero. It was found to be equal to $\varepsilon_g = 0.3$ eV.

The value of $r \approx 0.3$ for all samples (except samples doped with Se) says about essential role of acoustic and optic phonons in a scattering of electrons. The particularity of the concentration S_{11}dependence can be watched at $p \sim 1 \cdot 10^{20} cm^{-3}$, that would be also explain by influence of two-hole-subbands.

A computer simulation. Sb_2Te_3

A computer simulation of the Hall and Seebeck coefficients were carried out in the context of the two-subband model. We have solved numerically equations describing of the R_{ijk} (A16) and S_{ii} (A13), presented in our paper [1]

$$R_c = [A_c^{(1)} / p_0] \times [(t_a^{(1)})^2 / (1-\nu) + (t_a^{(2)})^2 / \nu\chi_c],$$
$$R_a = [A_a^{(1)} / p_0] \times [t_c^{(1)} t_a^{(1)} / (1-\nu) + (t_c^{(2)} t_a^{(2)})^2 / \nu\chi_a] \quad \text{A16)}$$

$$S_a = S_a^{(1)}(1-\nu) b_a / [(1-\nu) b_a + \nu] +$$
$$S_a^{(2)} \nu / [(1-\nu) b_a + \nu],$$
$$S_c = S_c^{(1)}(1-\nu) b_c / [(1-\nu) b_c + \nu] \quad \text{(A13)}$$
$$+ S_c^{(2)} \nu / [(1-\nu) b_c + \nu]$$

Here, we have the next notation: $\chi_c = A_c^{(1)} / A_c^{(2)}$, $\chi_a = A_a^{(1)} / A_a^{(2)}$, where χ_a and χ_c are the ratios of the structural Hall factors and $A_c^{(1)}, A_c^{(2)}, A_a^{(1)}, A_a^{(2)}$ are the structural Hall factors for bands 1 and 2 for $H \parallel \mathbf{c}$ and $H \perp \mathbf{c}$.

The calculation we made for the sample with $p = 1.2 \cdot 10^{20} cm^{-3}$ at T_0=100 K.

The next suppositions about a parameters of subbands were made. A part of these parameters were founded from experiments: $\varepsilon_v = \varepsilon_{v0} + \alpha T$; $\varepsilon_{v0} = 0{,}105 eV$; m_d/m_e (100) = 0.85; u_{a10}=700; u_{c10}=300; parameters of scattering r=0. And a part of parameters were founded by the comparison a calculating value of kinetic coefficients with experimental data: α =-0.4 10^{-4}eV/K;

$m_{dp1} = m_d/m_e$ (100)*(T/T_0).^0.08; m_{dp2}=0.1; b_a=0.85

$b_a = u_{a1}/u_{a2}$ ba=ua1/ua2; b_c=1/30 $b_c = u_{c1}/u_{c2}$;

parameters for Hall: A_c(100)= 0.75; A_a(100)=0.98;

$A_{a1} = A_a$(100)*(T/T_0)^(0);

$A_{c1} = A_c$(100)*(T/T_0)^0.3; χ_a=1; $\chi_a = A_{a1}/A_{a2}$;

χ_c=1; $\chi_c = A_{c1}/A_{c2}$ $u_{a1} = u_{a10}$*(T/T_0)^(-0.8);

$u_{c1} = u_{c10}$*(T/T_0)^(-0.8).

The results of the computer calculations for sample N 1 is presented on the Fig.3-4.

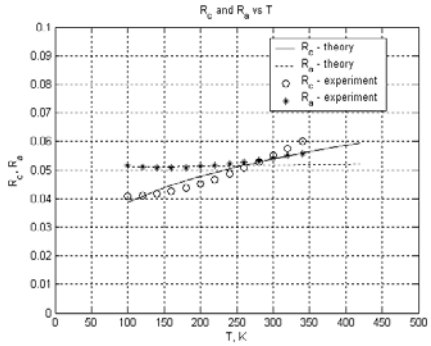

Fig.3 Experimental and calculating dependences of Rijk for the sample of Sb_2Te_3 crystal with $p = 1.2 \cdot 10^{20} cm^{-3}$.

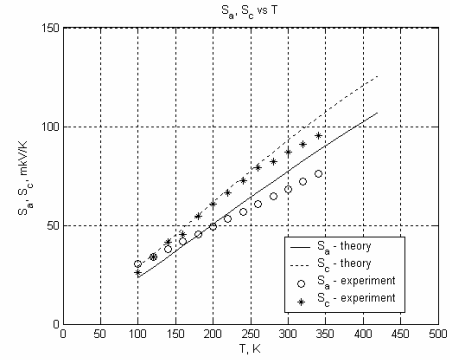

Fig.4. Experimental and calculating dependences of Sii for the sample of Sb_2Te_3 crystal with $p = 1.2 \cdot 10^{20} cm^{-3}$.

$Bi_{0,5}Sb_{1,5}Te_3$

The experimental results of the transverse Nernst-Ettingshausen tensor components and the Seebeck coefficients of $Sb_{1.5}Bi_{0.5}Te_3$ samples are presented on the Fig.5,6.

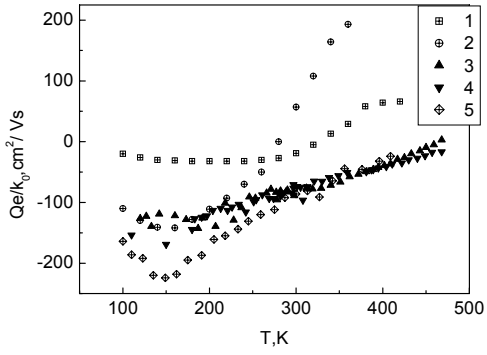

Fig. 5 Temperature dependences Qe/k_0 for monocrystalls of $Bi_{0,5}Sb_{1,5}Te_3$.

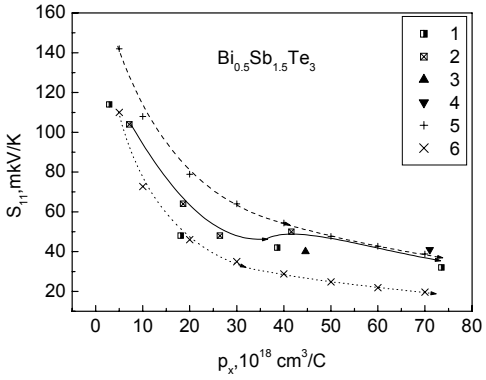

Fig.6. S_{11} - dependence on hole concentration p at T=120K. Points 1-4 are experimental data, points 5,6 – calculation for 1- zone model (5) and 2 – zone model (6) for r=0.

We can see that dependence S from hole concentration has the particularity at p = 3 10^{19} cm^{-3} (Fig 6), that can be explain by influence of two-hole-subbands.

A computer simulation $Bi_{0,5}Sb_{1,5}Te_3$

A computer simulation of the Hall and Seebeck coefficients were carried out in the context of the two-subband model. We have solved numerically equations describing of the R_{ijk} (A16) and S_{ii} (A13)

The calculation we made for the sample with p=4.4 $10^{19}cm^{-3}$ at T_0=100 K.

The next suppositions about a parameters of subbands were made. A part of these parameters were founded from experiments: $\varepsilon_v = \varepsilon_{v0} + \alpha T$; $\varepsilon_{v0} = 0,025eV$; m_d/m_e (100) = 0.4; u_{a10}=800; u_{c10}=500; parameters of scattering r=0. And a part of parameters were founded by the comparison a calculating value of kinetic coefficients with experimental data: α =-=-2.0e 10^{-5}eV/K;

m_{dp1}= m_d/m_e (100)*(T/T_0).^0.4; m_{dp2}=1; b_a=2 $b_a = u_{a1}/u_{a2}$; ba=ua1/ua2;bc =1/2; $b_c = u_{c1}/u_{c2}$;

parameters for Hall: $A_c(100)$= 0.55 ; $A_a(100)$=1; Aa1=Aa_100*(T/T0).^(0.25); Ac1=Ac_100*(T/T0).^(0.25); χ_a=1; $\chi_a = A_{a1}/A_{a2}$; χ_c=0.8; $\chi_c = A_{c1}/A_{c2}$ $u_{a1} = u_{a10}*(T/T_0)^{(-0.8)}$; $u_{c1} = u_{c10}*(T/T_0)^{(-0.8)}$.

Parameter of scattering r=0 The results of the computer calculations for sample with p=4.4 $10^{19}cm^{-3}$ is presented on the Fig.5-8.

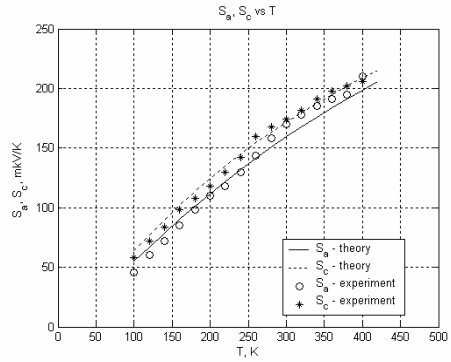

Fig.7. Experimental and calculating dependences of Sii for the sample $Bi_{0,5}Sb_{1,5}Te_3$ with p=4.4 $10^{19}cm^{-3}$.

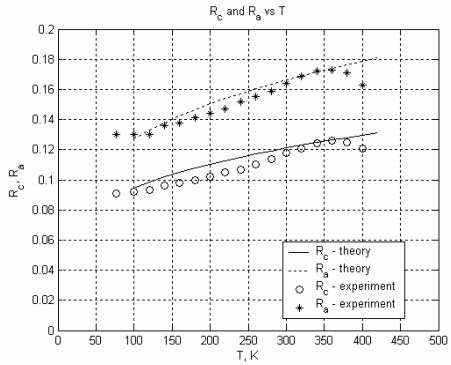

Fig.8. Experimental and calculating dependences of Rijk for the sample $Bi_{0,5}Sb_{1,5}Te_3$ with p=4.4 $10^{19}cm^{-3}$.

Our calculation supports the conception of the influence of two-band structure of valence band for Sb_2Te_3 and p-type solid solution $Sb_{1.5}Bi_{0.5}Te_3$.

Conclusions

We have shown that the experimental data on the monocrystals Sb_2Te_3 and p-type solid solution $Sb_{1.5}Bi_{0.5}Te_3$. can be explained within the two-band model of the valence band. Evaluation of the band-gap width ε_g and of the energy gap between the main and additional valence band extrema yielded for Sb_2Te_3 $\varepsilon_g \approx 0.3$ eV, $\Delta\varepsilon_v \approx 0.1$eV and for $Sb_{1.5}Bi_{0.5}Te_3$ $\varepsilon_g \approx 0.12$ eV, $\Delta\varepsilon_v \approx 0.02$ eV).

References

1. Zhitinskaya M.K., Nemov S.A., Ivanova L.D. "The Nernst-Ettingshausen, Seebeck and Hall Effects in Sb2Te3 Single Crystals", Russian. Solid State Physics, Vol.44, No.1 (2002), 41-46.

2 Langhammer.H.T., Stordeur M., Sobotta H., Riede V.,Physica Status Solidi(b),Vol.109,(1982),p.673-675.